Pure Steam Condensation Experiments on Nonisothermal Vertical Plates

H. J. H. Brouwers[1]
Akzo Research Laboratories Arnhem,
Fibers Division,
Department of Mechanical Engineering,
Arnhem, The Netherlands

Pure steam condensation experiments on flat channel plates have been performed. To provide a range of values of the governing groups NTU and Ad, steam was condensed crosscurrentwise on polyvinylidene fluoride (PVDF) plates and cocurrentwise on brass plates ($8.0\times10^{-6}\leq Ad\leq 8.4\times10^{-2}$, $0\leq NTU^{-1}\leq 10$). The theoretical predictions, based on an analysis of Nusselt-type condensation on nonisothermal plates, agree excellently with the plastic-plate measurements. The brass-plate experiments, however, agree with the theoretical model only in a limited range of NTU and Ad.

Introduction

Laminar film condensation of pure saturated vapors on vertical flat plates has often been examined in the past. Several extensions and improvements have been proposed to the original analysis of Nusselt (1916). Bromley (1952) and Rohsenow (1956) included the heat capacity of the condensate, Sparrow and Gregg (1959) extended this analysis to include the inertia of the condensate, and Koh et al. (1961) additionally analyzed the effect of vapor drag. Chen (1961), Koh (1961), and Churchill (1986) derived approximate solutions accounting for the aforesaid effects. Ünsal (1988) extended the classical Nusselt model with the effect of surface waves on the condensate. Brouwers (1989) considered the Nusselt condensation on nonisothermal plates. In this paper increases in temperature of the cooling liquid in a channel plate due to liberated latent heat were included. It was furthermore demonstrated that the co-, counter-, and crosscurrent processes are governed by NTU and Ad (see the nomenclature for definitions).

In order to validate the Nusselt condensation model, numerous pure vapor condensation experiments on isothermal plates have been reported, e.g., steam condensation by Slegers and Seban (1970). These efforts, however, were limited to experiments on flat isothermal plates, thus only verifying the special case $Ad=\infty$; see Brouwers (1989). Accordingly, pure steam condensation experiments have been carried out on brass and polyvinylidene fluoride (PVDF) channel plates for a wide range of NTU and Ad values. The results of these experiments are presented in this paper.

Apparatus

The low-pressure steam used is supplied by the central boilerhouse. Since the water has been degassed before boiling, it is not expected to contain any noncondensables. The steam has an absolute pressure P_v of 2.25 bar, with a corresponding saturation temperature T_{sat} of 124°C, and is somewhat superheated; $T_{v,in}=135$°C. This degree of superheat is, however, insignificant, e.g., see Sparrow and Eckert (1961) or Minkowycz and Sparrow (1966); hence the steam can be regarded as saturated. The steam enters a cylindrical chamber with thick (20 mm) PVDF walls to condense on four parallel channel plates; see Figs. 1 and 2. The distance between the plates is such that interactions between the condensation processes on the separate plates are excluded. The entire test chamber is thermally insulated with plastic foam to avoid undesired heat

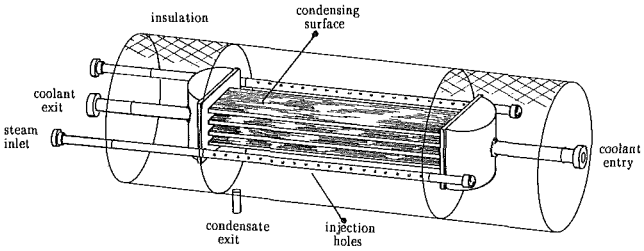

Fig. 1 Tested PVDF channel plates

	PVDF	brass
B_{tot} (mm)	40.2	40
d_1 (mm)	1.4	3.4
d_2 (mm)	1.6	3.4
d_3 (mm)	0.4	0.6
d_4 (mm)	0.3	0.3
d_5 (mm)	40	40
d_6 (mm)	2.0	4.0
k_w (W/mK)	0.19	85
$\bar{h}_w$ (W/m²K)	1266.6	$56.6\ 10^4$

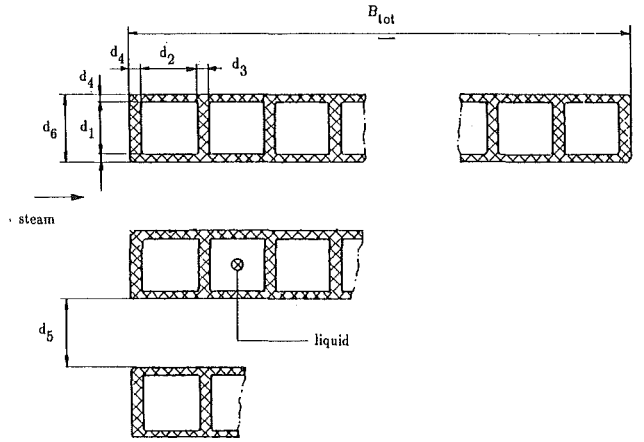

Fig. 2 Properties and dimensions of tested channel plates

[1]Present address: Twente University, Department of Civil Engineering, P.O. Box 217, 7500 AE Enschede, The Netherlands.

Contributed by the Heat Transfer Division for publication in the JOURNAL OF HEAT TRANSFER. Manuscript received by the Heat Transfer Division November 1990; revision received December 1991. Keywords: Condensation, Heat Exchangers, Mass Transfer.

loss. The entering coolant, i.e., water, has during the experiments an inlet temperature $T_{l,in}$ of about 11°C. The various temperatures of the test setup are measured with laboratory mercury thermometers, and the coolant flow with calibrated flowmeters.

At the start of the experiments, the condensate in the connecting tubes was removed by blowing through steam. By injecting steam, with zero coolant flow, the air present was driven out of the test chamber through a vent hole in the bottom.

In order to create two different McAdams numbers, both PVDF and brass (DIN Ms 63) channel plates have been tested. Because of the poor thermal conductivity of PVDF, the corresponding Ad was small. The difference with the larger Ad of the brass plate is furthermore increased by adapting the orientation of the setup with respect to the vertical: The vapor condenses cocurrentwise on the brass plates and crosscurrentwise on the PVDF plates. In Fig. 2 the dimensions of both setups are listed. The NTU is simply varied by adjusting the liquid mass flow through the plates, since NTU is inversely proportional to the liquid capacity flow through a plate.

Theory

To obtain NTU^{-1} and Ad, the physical properties of both fluids have to be determined. As these properties depend on temperature, the proper reference temperatures have to be calculated. The McAdams number is defined as:

$$\mathrm{Ad} = \frac{\bar{h}_{pl}^4 \eta_c (L \text{ or } B)(T_{\mathrm{sat}} - T_{l,in})}{16 \rho_c^2 H_{fg} k_c^3 g}. \tag{1}$$

For co- and countercurrent condensation, L should be used in this equation, while for crosscurrent condensation B should be considered, corresponding with the flow-off length of the processes concerned. The McAdams number is a measure of the ratio, to the fourth power, of the total heat transfer coefficient of the plate and the heat transfer coefficient of the condensate films. The total heat transfer coefficient of the plate $\bar{h}_{pl}$, appearing in Ad and NTU, is defined by:

$$\frac{1}{\bar{h}_{pl}} = \frac{1}{\bar{h}_w} + \frac{1}{\bar{h}_l}. \tag{2}$$

The heat transfer coefficient $\bar{h}_w$ of the walls follows from:

$$\bar{h}_w = 2\frac{k_w}{d_4}, \tag{3}$$

and is listed in Fig. 2. The heat transfer coefficient from channel plate to coolant follows from:

$$\bar{h}_l = \frac{2\overline{\mathrm{Nu}}_l k_l}{D_{h,l}} \left(\frac{\mathrm{Pr}_l}{\mathrm{Pr}_{l,w}} \right)^{0.11} \cong \frac{4\overline{\mathrm{Nu}}_l k_l}{(d_1 + d_2)} \left(\frac{\mathrm{Pr}_l}{\mathrm{Pr}_{l,w}} \right)^{0.11}. \tag{4}$$

In this paper the correlation of Dennis et al. (1959) ($\mathrm{Nu}_{l,\infty} = 2.98$) is employed for the average laminar convective flow Nusselt number because in both plates the flow remains in the laminar flow regime. This correlation only accounts for the effect of the thermal entry length, not the hydrodynamic. Neti and Eichhorn (1983) demonstrated numerically that the hydrodynamic development region has little effect for $\mathrm{Pr}_l > 6$ and $\mathrm{Re}_l \mathrm{Pr}_l D_{h,l}/L < 120$. As these conditions are satisfied in the tested channel plates, the correlation of Dennis et al. (1959) can be used. The factor of two in Eqs. (3) and (4) accounts for the heat transfer on both sides of the plate.

For the brass channel plates (unlike the plastic plates) the Nusselt number in Eq. (4) is furthermore multiplied by a factor of two to account for the heat transfer through the intermediate walls in the plate, which act as extra heat transfer surfaces. In Eq. (4) also the Sieder and Tate correction appears; see V.D.I. (1988). This correction is of minor importance for plastic plates since the temperature (and related dynamic viscosity) variation across the channels will be small; $\bar{h}_{pl}$ is dominated by $\bar{h}_w$ rather than by $\bar{h}_l$.

The physical properties of the coolant are evaluated at:

$$T_l^* = \frac{T_{l,in} + T_{l,\mathrm{out}}}{2}, \tag{5}$$

as suggested by V.D.I. (1988).

To calculate the coolant Prandtl number at the brass wall, $\mathrm{Pr}_{l,w}$, the temperature at the wall needs to be known; see Eq. (4). This temperature follows from the energy balance:

$$\bar{h}_w (T_{c,w}^* - T_{l,w}^*) = \bar{h}_l (T_{l,w}^* - T_l^*), \tag{6}$$

see Fig. 3. The mean wall reference temperature is derived from Eq. (6) as:

$$T_{l,w}^* = \frac{T_{c,w}^* \bar{h}_w + T_l^* \bar{h}_l}{\bar{h}_w + \bar{h}_l}. \tag{7}$$

The mean reference interface temperature $T_{c,w}^*$ at condensate-plate surface follows from the energy balance:

$$\bar{h}_{pl} (T_{c,w}^* - T_l^*) = \bar{h}_c (T_{\mathrm{sat}} - T_{c,w}^*). \tag{8}$$

This equation is rewritten to obtain the reference temperature:

Nomenclature

Ad = McAdams number $= \bar{h}_{pl}^4 \eta_c (L \text{ or } B)(T_{\mathrm{sat}} - T_{l,in})/16\rho_c^2 H_{fg} k_c^3 g$
B = net plate width, m
c_p = specific heat, $\mathrm{Jkg^{-1}K^{-1}}$
D_h = hydraulic diameter = four times the cross-sectional/the perimeter, m
d_i = geometric property of heat exchanger, see Fig. 2, m
g = acceleration due to gravity, $\mathrm{ms^{-2}}$
H_{fg} = latent heat of condensation, $\mathrm{Jkg^{-1}}$
h = heat transfer coefficient, $\mathrm{Wm^{-2}K^{-1}}$
Ku = Kutateladze number $= c_{p,c}(T_{\mathrm{sat}} - T_{c,w})/H_{fg}$
k = thermal conductivity, $\mathrm{Wm^{-1}K^{-1}}$
L = net plate length, m
M = Morton number $= g\eta_c^4/\sigma_c^3\rho_c$
$\dot{m}$ = local mass flux into condensate, $\mathrm{kgm^{-2}s^{-1}}$
NTU = number of transfer units $= \bar{h}_{pl} BL/w_l c_{p,l}$
Nu = Nusselt number $= hD_h/k$
P = pressure, bar
Pr = Prandtl number $= \eta c_p/k$
Q = dimensionless condensate formation $= (1 - \Theta_{\mathrm{out}})/\mathrm{NTU}$
Re_c = condensate flow Reynolds number $= w_c/2\eta_c(L \text{ or } B)$
Re_l = coolant flow Reynolds number $= w_l/\eta_l B$
T = temperature, K
w = mass flow, $\mathrm{kgs^{-1}}$
η = dynamic viscosity, Pas
Θ = dimensionless temperature $= (T_{\mathrm{sat}} - T_l)/(T_{\mathrm{sat}} - T_{l,in})$
ρ = density, $\mathrm{kgm^{-3}}$
σ = surface tension, $\mathrm{Nm^{-1}}$

Subscripts

c = condensate
in = entry
l = liquid in channel plate
out = exit
pl = channel plate
sat = saturation
tot = total
v = vapor
w = channel plate/coolant or channel plate/condensate interface
∞ = fully developed flow

Superscripts

$\bar{}$ = mean
* = reference

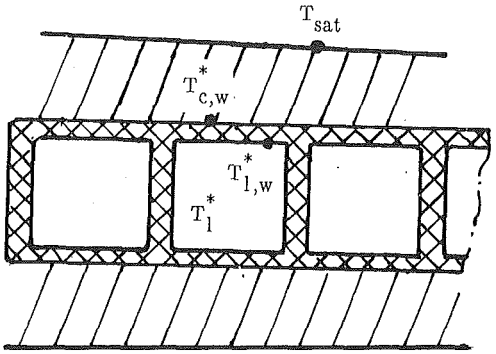

Fig. 3 Heat transfer from vapor-condensate surface to coolant

$$T^*_{c,w}=\frac{\bar{h}_c T_{sat}+\bar{h}_{pl}T^*_l}{\bar{h}_c+\bar{h}_{pl}}. \tag{9}$$

The mean heat transfer coefficient of the Nusselt condensation model reads:

$$\bar{h}_c=\frac{8}{3}\left[\frac{\rho_c^2 H_{fg}k_c^3 g}{4\eta_c(L \text{ or } B)(T_{sat}-T^*_{c,w})}\right]^{1/4}, \tag{10}$$

(which can, for instance, be found from Bird et al., 1960). For co- and countercurrent condensation, L should be employed in Eq. (10), while for crosscurrent condensation B should be used. Following Minkowycz and Sparrow (1966), the properties of the condensate are evaluated at reference temperature:

$$T^*_c=\frac{T_{sat}+2T^*_{c,w}}{3}, \tag{11}$$

except for H_{fg}, which is evaluated at T_{sat}. To determine $\bar{h}_l$ and $\bar{h}_c$, the reference temperatures $T^*_{l,w}$ and $T^*_{c,w}$ have to be known to determine the physical properties of both fluids. These heat transfer coefficients, however, depend on the physical properties. A successive substitution method is used to determine the matching $\bar{h}_l$, $\bar{h}_c$, $T^*_{l,w}$, and $T^*_{c,w}$. The $T^*_{c,w}$ thus determined is furthermore used to evaluate the physical properties of the condensate contained in Ad; see Eq. (11).

Results

In Figs. 4 and 5 the results of the experiments on brass and PVDF plate are depicted as a function of NTU^{-1}. In these figures also the theoretical Q and Θ_{out} predictions of Brouwers (1989) are plotted. The thin horizontal and vertical bars in both figures are the ranges of experimental uncertainty. The primary measurements of temperature and liquid flow introduce uncertainties in NTU, Θ_{out}, and Q, which are derived in the appendix.

The largest NTU^{-1} of the PVDF plates corresponds to $Re_l=993$ and $Re_c Pr_c^{0.95}=13$; consequently, both fluids are in the laminar flow regime (V.D.I., 1988). The maximum condensate Reynolds number follows from an overall mass balance of vapor entering the condensate films on both sides of the plate, w_c (by Brouwers, 1989, referred to as: M), and condensate flowing off the plate:

$$Re_c=\frac{w_c}{2\eta_c(L \text{ or } B)}, \tag{12}$$

where L should be used for crosscurrent condensation and B for co- and countercurrent condensation. For crosscurrent condensation, however, the produced condensate and Re_c varies with the distance from the entry of the coolant; the maximum condensate mass flux is found where the coolant enters the plate. The local mass flux times latent heat of condensation equals the heat flux from vapor-condensate surfaces to coolant. The local mass flux into the films is highest if the heat

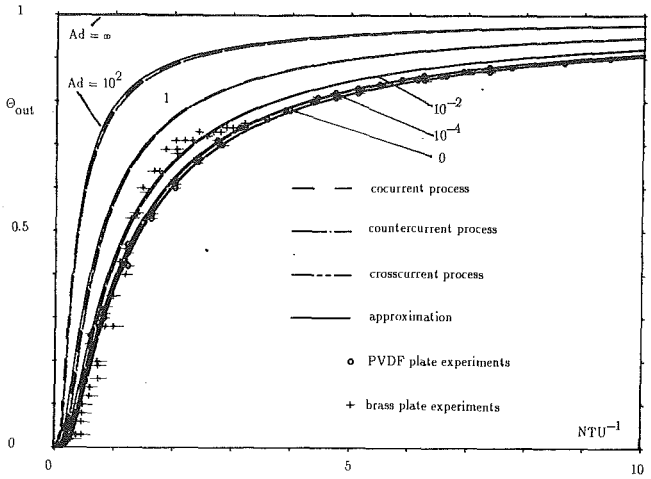

Fig. 4 Theoretical (Brouwers, 1989) and experimental variation of Θ_{out} with NTU^{-1}

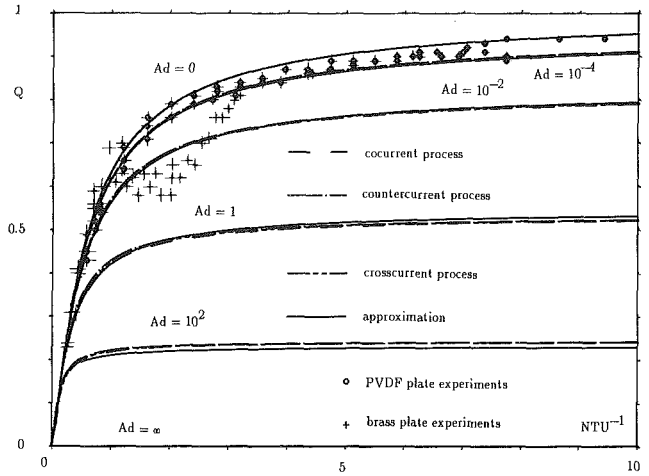

Fig. 5 Theoretical (Brouwers, 1989) and experimental variation of Q with NTU^{-1}

resistance of the film is neglected. Hence, an overestimation of Re_c is obtained when

$$w_c=LB\dot{m}<LB\,\frac{\bar{h}_{pl}(T_{sat}-T_{l,in})}{H_{fg}} \tag{13}$$

is substituted into Eq. (12). Combining Eqs. (12) and (13) results in said maximum value $Re_c Pr_c^{0.95}=13$ for the PVDF experiments.

The Ad of the PVDF experiments increased with rising NTU^{-1} from 0.8×10^{-5} to 1.1×10^{-5}. This minor variation is due to the poor heat transfer coefficient of the plastic walls; $\bar{h}_w=1266.6$ W/m^{2}K (see Fig. 2). Although the heat transfer from coolant to wall is enhanced by larger mass flows, entry effects cause a $\bar{h}_l$ range from 2600 W/m^{2}K to 3800 W/m^{2}K, and $\bar{h}_{pl}$ and Ad remain dominated by $\bar{h}_w$. Figures 4 and 5 illustrate the excellent agreement between experiment and theory, which predicts hardly any influence of the formed condensate on heat transfer for small values of Ad. Note that $Ad\simeq0$ represents a limiting case of the analysis of Brouwers (1989) (the other one is: $Ad=\infty$), which has never been examined experimentally.

In both figures the experimental results of the condensation on the brass plate are also presented as a function of NTU^{-1}. The largest NTU^{-1} in these plots, $NTU^{-1}=3.2$, corresponds to maximum $Re_l=2218$ and $Re_c Pr_c^{0.95}=209$, so that laminar

coolant and condensate flow are guaranteed. The maximum Reynolds number Re_c of the condensate is obtained using Eq. (12) with B applied. The thickness of the condensate films flowing off the plates is one-dimensional for co- and countercurrent condensation. Hence w_c need not be assessed with Eq. (13), but follows readily from the overall energy balance:

$$w_c H_{fg} = w_l c_{p,l}(T_{l,\text{out}} - T_{l,in}). \quad (14)$$

The subcooling of the condensate is neglected in Eq. (14), which is allowed for small Ku.

During the experiments $\bar{h}_l$ increased from 2600 W/m^{2}K to 5600 W/m^{2}K with increasing NTU^{-1} owing to entry effects. As $\bar{h}_l$ dominates $\bar{h}_{pl}$ (see Eq. (2) and note that $\bar{h}_w = 566{,}000$ W/m^{2}K (Fig. 2)), $\bar{h}_{pl}$ and Ad rise almost to the same extent as $\bar{h}_l$: Ad increased from 0.29×10^{-2} to 8.4×10^{-2} with increasing coolant flow.

Figures 4 and 5 illustrate the departure from the theory for very small and large NTU^{-1}. The discrepancy for very small NTU^{-1} is attributed to the contribution of unavoidable leakage heat flows to the coolant in the brass headers (the PVDF plates were fitted in thermally well-insulating PVDF headers). Accordingly, unreasonably high exit temperatures are measured. Some Θ_{out} even lie below the curve pertaining to Ad = 0, which is physically impossible. Beyond $NTU^{-1} = 2$ the experimental exit temperatures lie between the curves Ad = 0 and Ad = 10^{-2}, and are thus in agreement with the theoretical prediction. However, for $NTU^{-1} > 2$, the experimental Θ_{out} intersects the curve Ad = 10^{-2} and tends to approach the curve Ad = 0, although the experimental Ad approximates 8.4×10^{-2}. This implies that the measured value of Θ_{out} is smaller than predicted, that is to say, the calculated exit temperature is too low. The heat transfer from vapor to coolant is apparently better than predicted by the model. Three possible departures from the ideal model conditions are:

- ripples on the condensate surface,
- dropwise condensation,
- forced vapor flow in the test chamber.

In the literature the appearance of ripples is often quoted as a major explanation of the Nusselt condensation model underestimating the heat transfer from condensate to wall. For all experiments the dimensionless combination Ku/Pr_c was much smaller than 0.1. This implies that the results of the model of Ünsal (1988) can be applied (Ku/Pr_c is referred to as F in this note).

In Ünsal's paper the heat transfer through a condensate film with ripples is compared with that through a film without ripples: the Nusselt solution. One of the results relevant here is that for $4Re_c = 400$, the heat transfer from condensate to plate is augmented by ripples by at most a factor of 1.5; see Fig. 6 for a comparison with Nusselt's solution. An additional requirement for this value to be attained is that the Morton number M be larger than 1.06×10^{-12}. For all condensation experiments, however, this number proved to be of the order of 0.16×10^{-12}, so the effect of surface ripples should be less pronounced.

In Fig. 6 experimental data of Ratiani and Shekriladze (1964) are also shown, as well as the heat transfer coefficient of Nusselt's model and its corrected expression for the effect of waves following Kutateladze and Gogonin (1979):

$$\bar{h}_c = \frac{8}{3}\left[\frac{\rho_c^2 H_{fg} k_c^3 g}{4\eta_c (L \text{ or } B)(T_{\text{sat}} - T_{c,w})}\right]^{1/4} \text{Re}_c^{0.04}, \quad (15)$$

where Re_c is the maximum Reynolds number of the condensate and $T_{c,w}$ the constant temperature of the isothermal plate. For condensation on isothermal plates the maximum condensate Reynolds number reads:

$$\text{Re}_c = \frac{\rho_c^2 k_c g}{3\eta_c^2}\left[\frac{\rho_c^2 H_{fg} k_c^3 g}{4\eta_c (L \text{ or } B)(T_{\text{sat}} - T_{c,w})}\right]^{-3/4}. \quad (16)$$

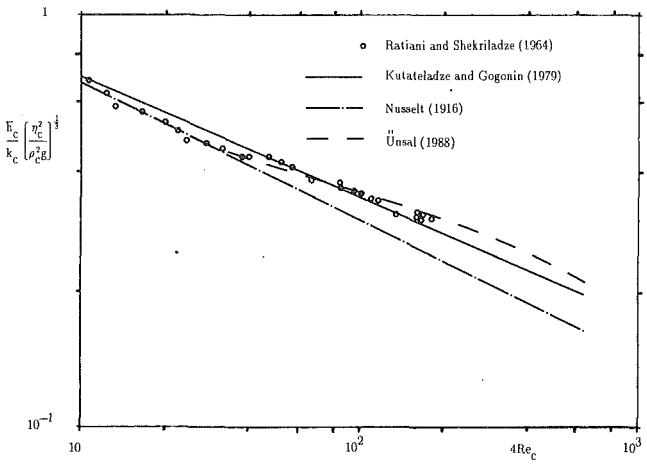

Fig. 6 Condensation heat transfer according to Nusselt (1916), Ünsal (1988), Ratiani and Shekriladze (1964), and Kutateladze and Gogonin (1979)

Ünsal (1988) refers to Re_c as "$\overline{Re}_L$" (for "$\overline{Re}_L^{1/3}$" in Eq. (13) of this paper one should read "$\overline{Re}_L^{1/3}$"). Figure 6 illustrates the fair agreement between the result of the comprehensive analysis of Ünsal (1988), the compact correction suggested by Kutateladze and Gogonin (1979), and experiments reported by Ratiani and Shekriladze (1964). However, all experimental and theoretical results indicate that ripples alone cannot explain why the calculated heat transfer is so poor. For when Ad is divided by 5, corresponding with the suspected effect of waves to the fourth power, the calculated exit temperature is still too low.

During the experiments it was not possible to watch the plates and verify whether film condensation actually occurred. However, the experimental and theoretical results indicate that the discrepancy between the results depends on the coolant mass flow (and related condensation rate), revealing that the deviation cannot be explained by possible dropwise condensation only. Moreover, dropwise condensation is not expected because the brass plates do not have smooth and clean surfaces. They are constructed from square channels joined by soldering.

The amount of steam injected into the test chamber and condensed on the plates increases with higher coolant flow rates. For the brass plate experiments the maximum steam mass flow amounts to 44 kg/h, owing to the excellent heat transfer in this plate. Although the steam is injected by two injectors, provided with many holes turned away from the channel plates, it is suspected that the condensate films are disturbed, or even blown off the plates, by the incoming steam. In general, forced convection reduces the condensate film thickness and hence also the related heat resistance of the film. Enhanced heat transfer through the film leads to a small experimental Ad. The experimental data indeed approximate the theoretical curves for Ad = 10^{-2} and Ad = 10^{-4} (note that Ad = 0 corresponds physically to a negligible/absent film).

The effect of forced flow in the test chamber was also regarded by Slegers and Seban (1970) as the most acceptable explanation for their experimental results being 20 percent above theory. For that matter, during their experiments the maximum amount of injected steam was only about 1 kg/h.

For the PVDF plate the steam flow reaches a maximum rate of 9 kg/h. It is conceivable that here, too, film heat transfer is enhanced by forced steam flow. This cannot be observed because even for ideal Nusselt condensation the film is negligible (since Ad ≃ 0). However, good agreement between theory and experiments is also found for small coolant (and related vapor and condensate) flow rates. Accordingly, one can assume that at least for small coolant (and vapor mass) flows, where

Nusselt condensation is ensured, theory and experiment are in agreement.

Conclusions

In the past the Nusselt condensation model has only been compared with isothermal plate and tube condensation experiments ($Ad \simeq \infty$). Based on the assumption of Nusselt type condensation, which has been thoroughly verified, pure steam condensation experiments have been carried out on nonisothermal plates. Crosscurrent condensation experiments performed on PVDF channel plates ($Ad \simeq 10^{-5}$, $0 \leq NTU^{-1} \leq 10$) confirm that the predictions of Brouwers (1989) are essentially correct. The thermal conductivity of these plates is such that it entirely dominates the heat transfer (the film can be regarded as isothermal or absent).

The theoretical predictions of cocurrent condensation on brass plates correspond with experiments ($0.29 \times 10^{-2} \leq Ad \leq 8.4 \times 10^{-2}$, $0 \leq NTU^{-1} \leq 3.2$) only in a limited range of both governing dimensionless groups NTU and Ad. Complete agreement with the model might have been obtained if perfect thermal insulation and quiescent vapor conditions had been more nearly achieved.

Acknowledgments

The author thanks the management of Akzo Research Laboratories Arnhem for their permission to publish this paper and Messrs. H. P. Korstanje and G. Vegt for their support. He also expresses his gratitude to Prof. A. K. Chesters of Eindhoven University of Technology for his stimulating discussion on the subject.

References

Bird, R. B., Stewart, W. E., and Lightfoot, E. N., 1960, *Transport Phenomena*, Wiley, New York.

Bromley, L. A., 1952, "Effect of Heat Capacity of Condensate," *Ind. Eng. Chem.*, Vol. 44, pp. 2966-2969.

Brouwers, H. J. H., 1989, "Film Condensation on Non-isothermal Vertical Plates," *Int. J. Heat Mass Transfer*, Vol. 32, pp. 655-663.

Chen, M. M., 1961, "An Analytical Study of Laminar Film Condensation: Part 1—Flat Plates," ASME JOURNAL OF HEAT TRANSFER, Vol. 83, pp. 48-54.

Churchill, S. W., 1986, "Laminar Film Condensation," *Int. J. Heat Mass Transfer*, Vol. 29, pp. 1219-1226.

Dennis, S. R. C., Mercer, A. M., and Poats, G., 1959, "Forced Heat Convection in Laminar Flow Through Rectangular Ducts," *Quart. Appl. Math.*, Vol. 17, pp. 285-297.

Holman, J. P., 1978, *Experimental Methods for Engineers*, 3rd ed., McGraw-Hill, New York.

Kline, S. J., and McClintock, F. A., 1953, "Describing Uncertainties in Single-Sample Experiments," *Mech. Eng.*, Vol. 75, pp. 3-8.

Koh, J. C. Y., 1961, "On Integral Treatment of Two-Phase Boundary Layer in Film Condensation," ASME JOURNAL OF HEAT TRANSFER, Vol. 83, pp. 359-362.

Koh, J. C. Y., Sparrow, E. M., and Hartnett, J. P., 1961, "The Two Phase Boundary Layer in Laminar Film Condensation," *Int. J. Heat Mass Transfer*, Vol. 2, pp. 69-82.

Kutateladze, S. S., and Gogonin, I. I., 1979, "Heat Transfer in Film Condensation of Slowly Moving Vapor," *Int. J. Heat Mass Transfer*, Vol. 22, pp. 1593-1599.

Minkowycz, W. J., and Sparrow, E. M., 1966, "Condensation Heat Transfer in the Presence of Noncondensables, Interfacial Resistance, Superheating, Variable Properties, and Diffusion," *Int. J. Heat Mass Transfer*, Vol. 9, pp. 1125-1144.

Neti, S., and Eichhorn, R., 1983, "Combined Hydrodynamic and Thermal Development in a Square Duct," *Num. Heat Transfer*, Vol. 6, pp. 497-510.

Nusselt, W., 1916, "Die Oberflächenkondensation des Wasserdampfes," *Z. Ver. dt. Ing.*, Vol. 60, pp. 541-546, 569-575 [in German].

Ratiani, G. V., and Shekriladze, I. G., 1964, "An Experimental Study of the Heat Exchange Process on Transition From Laminar to Turbulent Flow of the Film," *Thermal Engng.*, Vol. 11, pp. 101-102.

Rohsenow, W. M., 1956, "Heat Transfer and Temperature Distribution in Laminar-Film Condensation," *Trans. ASME*, Vol. 78, pp. 1645-1648.

Slegers, L., and Seban, R. A., 1970, "Laminar Film Condensation of Steam Containing Small Concentrations of Air," *Int. J. Heat Mass Transfer*, Vol. 13, pp. 1941-1947.

Sparrow, E. M., and Gregg, J. L., 1959, "A Boundary Layer Treatment of Laminar-Film Condensation," *Trans. ASME*, Vol. 81, pp. 13-17.

Sparrow, E. M., and Eckert, E. R. G., 1961, "Effects of Superheated Vapor and Noncondensable Gases on Laminar Film Condensation," *AIChE Journal*, Vol. 7, pp. 473-477.

Ünsal, M., 1988, "Effect of Waves on Nusselt Condensation," *Int. J. Heat Mass Transfer*, Vol. 31, pp. 1944-1947.

V.D.I., 1988, *V.D.I.—Wärmeatlas*, 5. Aufl., V.D.I. Verlag GmbH [in German].

APPENDIX

Uncertainty Analysis

The uncertainty analysis presented here follows the procedures described by Kline and McClintock (1953) and Holman (1978). The primary experimental data, such as $T_{l,in}$, w_l, $T_{l,out}$, etc., are used to calculate the desired dimensionless quantities NTU, Θ_{out}, and Q. The uncertainty in these calculated results is obtained by considering the uncertainties in the primary measurements and is discussed below.

The uncertainty in a calculated result I, which is a function of the independent variables $i_1, i_2, \ldots, i_n$, reads:

$$\left(\frac{dI}{I}\right)^2 = \left(\frac{\partial I}{\partial i_1}\frac{di_1}{I}\right)^2 + \left(\frac{\partial I}{\partial i_2}\frac{di_2}{I}\right)^2 + \ldots + \left(\frac{\partial I}{\partial i_n}\frac{di_n}{I}\right)^2, \quad \text{(A1)}$$

where $di_1, di_2, \ldots, di_n$ represent the uncertainties in the quantities $i_1, i_2, \ldots, i_n$. Applying Eq. (A1) to Θ_{out} gives:

$$\left(\frac{d\Theta_{out}}{\Theta_{out}}\right)^2 = \left(\frac{dT_{l,in}}{T_{sat} - T_{l,in}}\right)^2 + \left(\frac{dT_{l,out}}{T_{sat} - T_{l,out}}\right)^2 + \left[\frac{(T_{l,out} - T_{l,in})\,dT_{sat}}{(T_{sat} - T_{l,in})(T_{sat} - T_{l,out})}\right]^2. \quad \text{(A2)}$$

This expression constitutes the relative uncertainty in Θ_{out} as a result of the uncertainties in the measured $T_{l,in}$, $T_{l,out}$, and T_{sat}, represented by $dT_{l,in}$, $dT_{l,out}$, and dT_{sat}, respectively. These temperatures are measured with mercury thermometers with inaccuracies of 0.1°C. The maximum $d\Theta_{out}$ amounts to 0.13×10^{-2} and 0.12×10^{-2} for the brass and PVDF experiments, respectively.

The uncertainty in NTU, denoted by dNTU, depends on dw_l, $dc_{p,l}$, dk_l, dk_p, dL, dB, dd_1, dd_2, and dd_4, see Eqs. (2), (3), and (4). Neglecting uncertainties in the physical and geometric properties, which are much smaller than the uncertainty of the liquid mass flow, Eq. (A1) produces:

$$\left(\frac{d\text{NTU}}{\text{NTU}}\right) = \left(\frac{dw_{g,in}}{w_{g,in}}\right). \quad \text{(A3)}$$

The total liquid mass flow is measured with the aid of a rotameter with an inaccuracy $4dw_l$ of 0.015 kg/s (the factor of 4 is introduced because the water is divided over 4 channel plates). For the experimental data of Figs. 3 and 4, the maximum dNTU amounts to 0.122 and 0.072 for the brass and PVDF experiments, respectively.

The uncertainty in Q depends on both the uncertainties in Θ_{out} and NTU. Applying Eq. (A1) yields:

$$\left(\frac{dQ}{Q}\right)^2 = \left(\frac{d\Theta_{out}}{1 - \Theta_{out}}\right)^2 + \left(\frac{d\text{NTU}}{\text{NTU}}\right)^2, \quad \text{(A4)}$$

where both $d\Theta_{out}$ and dNTU readily follow from Eqs. (A2) and (A3), respectively. For the brass experiments the maximum dQ reads 0.120, and for the PVDF experiments the maximum dQ amounts to 0.049.